BREACH: AN EROSION MODEL FOR EARTHEN DAM FAILURES

by D. L. Fread[1]

July 1988
(Revision 1, August 1991)

ABSTRACT. A physically based mathematical model (BREACH) to predict the breach characteristics (size, time of formation) and the discharge hydrograph emanating from a breached earthen dam is presented. The earthen dam may be man-made or naturally forme by a landslide. The model is developed by coupling the conservation of mass of the reservoir inflow, spillway outflow, and breach outflow with the sediment transport capacity of the unsteady uniform flow along an erosion-formed breach channel. The bottom slope o the breach channel is assumed to be essentially that of the downstream face of the dam. Tl growth of the breach channel is dependent on the dam's material properties (D_{50} size, unit weight, friction angle, cohesive strength). The model considers the possible existence of th following complexities: 1) core material having properties which differ from those of the outer portions of the dam; 2) the necessity of forming an eroded ditch along the downstrea face of the dam prior to the actual breach formation by the overtopping water; 3) the downstream face of the dam can have a grass cover or be composed of a material of larger grain size than the outer portion of the dam; 4) enlargement of the breach through the mechanism of one or more sudden structural collapses due to the hydrostatic pressure force exceeding the resisting shear and cohesive forces; 5) enlargement of the breach width by slope stability theory; 6) initiation of the breach via piping with subsequent progression to a free surface breach flow; and 7) erosion transport can be for either noncohesive (granular) materials or cohesive (clay) materials. The outflow hydrograph is obtained through a time-stepping iterative solution that requires only a few seconds for computation on a mainframe computer. The model is not subject to numerical stability or convergence difficulties. The model's predictions are compared with observations of a piping failure of the man-made Teton Dam in Idaho, the piping failure of the man-made Lawn Lake Dam in Colorado, and breached landslide-formed dam in Peru. Also, the model has been used to predict possible downstream flooding from a potential breach of the landslide blockage of Spirit Lake in the aftermath of the eruption of Mount St. Helens in Washington. Model sensitivity to numerical parameters is minimal; however, it is sensitive to the internal friction angle of th dam's material and the extent of grass cover when simulating man-made dams and to the cohesive strength of the material composing landslide-formed dams.

---

[1] Senior Research Hydrologist with the Hydrologic Research Laboratory, National Weather Service, NOAA, Silver Spring, Maryland 20910

INTRODUCTION

Earthen dams are subject to possible failure from either overtopping or piping water which erodes a trench (breach) through the dam. The breach formation is gradual with respect to time, and its width, as measured along the crest of the dam, usually encompasses only a portion of the dam's crest length. In many instances, the bottom of the breach progressively erodes downward until it reaches the bottom of the dam; however, in some cases, it may cease its downward progression at some intermediate elevation between the top and bottom of the dam. The size of the breach, as constituted by its depth and its width (which may be a function of the depth), and the rate of the breach formation determine the magnitude and shape of the resulting breach outflow hydrograph. This is of vital interest to hydrologists and engineers concerned with real-time forecasting or evacuation planning for floods produced by dam failures.

This paper presents a mathematical model (BREACH) for predicting the breach characteristics (size, shape, time of formation) and the breach outflow hydrograph. The model is physically based on the principles of hydraulics, sediment transport, soil mechanics, the geometric and material properties of the dam, and the reservoir properties (storage volume, spillway characteristics, and time-dependent reservoir inflow rate). The dam may be either man-made or naturally formed as a consequence of a landslide. In either, the mechanics of breach formation are very similar, the principal difference being one of scale. The landslide-formed dam is often much larger than even the largest of man-made earthen dams as illustrated in Fig. 1. The critical material properties of the dam are the internal friction angle, cohesive strength, and average grain size diameter (D_{50}).

The breach erosion model presented herein is a modification of an earlier version first reported by the author (Fread, 1984). The BREACH Model predicts a dam-breach outflow hydrograph. It differs from the parametric approach which the author has used in the NWS DAMBRK Model (Fread, 1977, 1981, 1983). The parametric model uses empirical observations of previous dam failures such as the breach width-depth relation, time of breach formation, and depth of breach to develop the outflow hydrograph. The breach erosion model presented herein can provide some advantages over the parametric breach model for application to man-made dams since the critical properties used by the model are measurable or can be estimated within a reasonable range from a qualitative description of the dam materials. However, it should be emphasized that, even if the properties can be measured, there is a range for their probable value, and within this range, outflow hydrographs of varying magnitude and shape will be produced by the model. The hydrologist or engineer should investigate the most critical combination of values for the dam's material properties. It is considered essential when predicting breach outflows of landslide dams to utilize a physically based model since observations of such are essentially nonexistent, rendering the parametric approach infeasible.

In this paper, the breach erosion model is applied to the piping initiated failures of the man-made Teton Dam in Idaho and the Lawn Lake Dam in Colorado; the overtopping failure

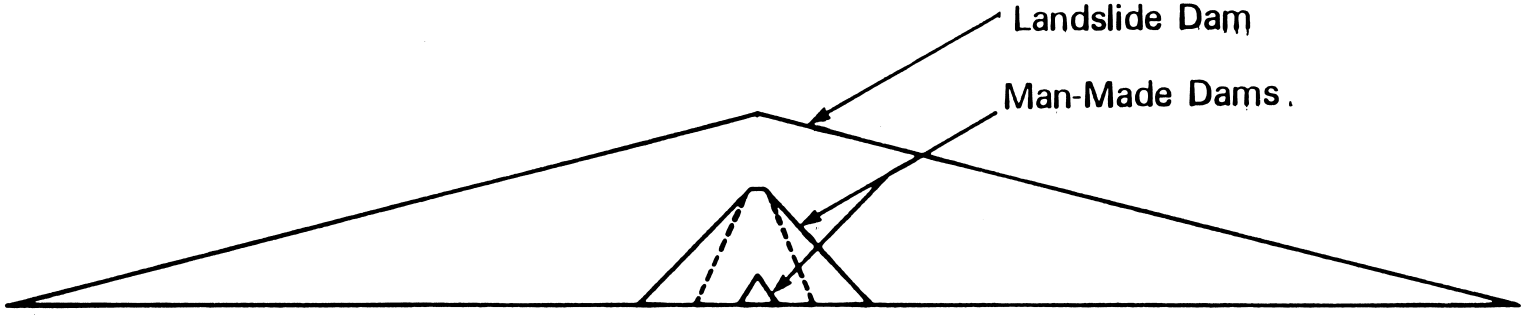

Figure 1. Comparative View of Natural Landslide Dams and Man-Made Dams

of the Mantaro landslide-formed dam in Peru; and the possible failure of the landslide blockage of Spirit Lake near Mount St. Helens in Washington.

PREVIOUS RESEARCH

Other investigators of dam breach outflows have developed physically based models.

The first was Cristofano (1965) who derived an equation which related the force of the flowing water through the breach to the shear strength of the soil particles on the bottom of the breach and, in this manner, developed the rate of erosion of the breach channel as a function of the rate of change of water flowing through the breach. He assumed the breach bottom width to be constant with time and always of trapezoidal shape in which the side slopes of the trapezoid were determined by the angle of repose of the breach material, and the bottom slope of the breach channel was equal to the internal friction angle of the breach material. An arbitrary empirical coefficient, which was critical to the model's prediction, was also utilized.

Harris and Wagner (1967) used the Schoklitsch sediment transport equation and considered the breach to commence its downward progression immediately upon overtopping, and the erosion of the breach was assumed to progress to the bottom of the dam. Brown and Rogers (1977) presented a breach model which was based on the work of Harris and Wagner.

Most recently Ponce and Tsivoglou (1981) presented a rather computationally complex breach erosion model which coupled the Meyer-Peter and Muller sediment transport equation to the one-dimensional differential equations of unsteady flow and sediment conservation. Reservoir storage depletion was included in the upstream boundary equation used in conjunction with the unsteady flow equations. The set of differential equations was solved with a four-point implicit finite difference scheme. Flow resistance was represented through use of the Manning n. Breach width was empirically related to the rate of breach flow. A small rivulet was assumed to be initially present along the flow path. "Outflow at start of the computation is a function of the assumed initial size of the rivulet. Progressive erosion widens and deepens the rivulet, increasing outflow and erosion rate in a self-generating manner. The upper cross-section on the sloping downstream face creeps upstream across the dam top until it reaches the upstream face, whereby rate of flow and erosion increase at a faster rate. If outflow increases enough to lower the reservoir level faster than the channel bed erodes, both outflow and erosion gradually diminish. Of course, outflow will eventually decrease even if the breach bed erodes all the way down to the stream bed. This mode of failure creates the outflow hydrograph in the shape of a sharp but nevertheless gradual flood wave." Ponce and Tsivoglou compared the model's predictions with observations of a breached landslide-formed dam on the Mantaro River in Peru. The results were considered good. However, they were influenced by the judicious selection of the Manning n, the breach width-flow relation parameter, and a coefficient in the sediment

transport equation, although Ponce and Tsivoglou stated that the selected values were within each one's reasonable range of variation. Also, problems of a numerical computational nature were alluded to in connection with solving the implicit finite difference unsteady flow equations. They also implied that further work was needed to improve the breach width-flo relation and in developing a relation between the Manning n and the hydraulic/sediment characteristics of the breach channel.

The breach erosion model presented in this paper differs substantially from those previously reported. A summation of the important differences will be given after the mode has been completely described in the next section.

MODEL DESCRIPTION

General

The breach erosion model (BREACH) simulates the failure of an earthen dam as shown in Fig. 2. The dam may be homogeneous or it may consist of two materials: an outer zone with distinct material properties (ϕ - friction angle, C - cohesion, D_{50} - average grain size (mm), and γ - unit weight), and an inner core with its ϕ, C, D_{50}, and γ values. Also, the downstream face of the dam may be specified as having: 1) a grass cover with specified length of either good or fair stand, 2) material identical to the outer portion of the dam, or 3) material of larger grain size than the outer portion. The geometry of the downstream face of the dam is described by specifying the top of the dam (H_u), the bottom elevation of the dam (H_f) or original streambed elevation, and its slope as given by the ratio 1 (vertical) : ZD (horizontal). Then, the geometry of the upstream face of the dam is described by specifying its slope as the ratio 1 (vertical) : ZU (horizontal). If the dam is man-made, it is further described by specifying a flat crest width (W_{cr}) and a spillway rating table of spillway flow vs. head on the spillway crest. Naturally formed landslide dams are assumed to <u>not</u> have a flat crest or, of course, a spillway.

The storage characteristics of the reservoir are described by specifying a table of surface area (S_a) in units of acre-ft vs. water elevation, the initial water surface elevation (H_i at the beginning of the simulation, and a table of reservoir inflows (Q_i) in cfs vs. the hour of their occurrence (T_i).

If an overtopping failure is simulated, the water level (H) in the reservoir must excee the top of the dam before any erosion occurs. The first stages of the erosion are only along the downstream face of the dam as denoted by the line A-A in Fig. 2 where, initially if no grass cover exists, a small rectangular-shaped rivulet is assumed to exist along the face. An erosion channel of depth-dependent width is gradually cut into the downstream face of the dam. The flow into the channel is determined by the broad-crested weir relationship:

$$Q_b = 3\ B_o(H-H_c)^{1.5} \qquad (1$$

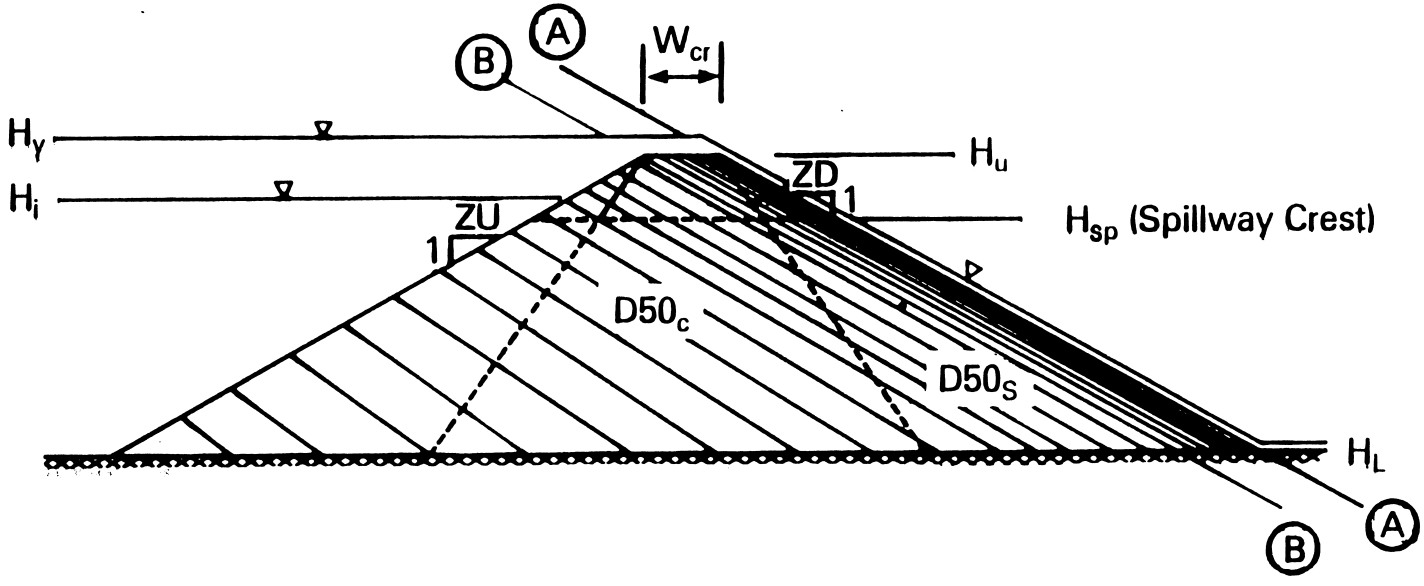

Figure 2. Side View of Dam Showing Conceptualized Overtopping Failure Sequence

in which Q_b is the flow into the breach channel, B_o is the instantaneous width of the initially rectangular-shaped channel, and H_c is the elevation of the breach bottom. As the breach erodes into the downstream face of the dam, the breach bottom elevation (H_c) remains at the top of the dam (H_u), and the most upstream point of the breach channel moves across the crest of the dam towards the dam's upstream face. When the bottom of the erosion channel has attained the position of line B-B in Fig. 2, the breach bottom (H_c) starts to erode vertically downward. The breach bottom is allowed to progress downward until it reaches the bottom elevation of the dam H_ℓ.

If the downstream face of the dam (line A-A in Fig. 2) has a grass cover, the velocity (v) of the overtopping flow along the grassed downstream face is computed at each time step by the Manning equation. This velocity is compared with a specified maximum permissible velocity (VMP) for grass-lined channels (see Chow, 1959). Failure of the downstream face via erosion is initiated at the time when the permissible velocity is exceeded. At that time a single rivulet having dimensions of one (ft) depth x two width is instantly created along the downstream face. Erosion within the rivulet is allowed to proceed as in the case where a grass cover does not exist. The velocity (v) along the downstream face is computed as follows:

$$q = 3(H-H_c)^{1.5} \qquad (1)$$

$$y = \left[\frac{qn'}{1.49(1/ZD)^{0.5}}\right]^{0.6} \qquad (2)$$

$$n' = aq^b \qquad (3)$$

$$v = q/y \qquad (4)$$

in which q is the overtopping flow per foot of crest length, $(H-H_c)$ is the hydrostatic head (f over the crest, n' is the Manning coefficient for grass-lined channels (Chow, 1959), a and b are fitting coefficients required to represent in mathematical form the graphical curves given in Chow.

If a piping breach is simulated, the water level (H) in the reservoir must be greater than the assumed center-line elevation (H_p) of the initially rectangular-shaped piping channel before the size of the pipe starts to increase via erosion. The bottom of the pipe is eroded vertically downward while its top erodes at the same rate vertically upwards. The flow into the pipe is controlled by orifice flow, i.e.,

$$Q_b = A\,[2g(H-H_p)/(1 + fL/D)]^{0.5} \qquad (5)$$

in which Q_b is the flow (cfs) through the pipe, g is the gravity acceleration constant, A is the cross-sectional area (ft^2) of the pipe channel, $(H-H_p)$ is the hydrostatic head (ft) on the pipe,

L is the length (ft) of the pipe channel, D is the diameter or width (ft) of the pipe, and f is the Darcy friction factor computed from the following mathematical representation of the Moody curves (Morris and Wiggert, 1972):

$$f = 64/N_R \quad \ldots\ldots\ldots \quad N_R < 2000 \tag{7}$$

$$f = 0.105 \left[\frac{D_{50}}{D}\right]^{0.167} \quad \ldots \quad N_R \geq 2000$$

$$N_R = 83333\, Q_b\, D/A \tag{9}$$

in which f is the Darcy friction factor and N_R is the Reynolds number. As the top elevation (H_{pu}) of the pipe erodes vertically upward, a point is reached when the flow changes from orifice-control to weir-control when the head on the pipe is less than the pipe diameter. The transition is assumed to occur when the following inequality is satisfied:

$$H < H_p + 2(H_{pu} - H_p) \tag{10}$$

The weir flow is then governed by Eq. (1) in which H_e is equivalent to the bottom elevation of the pipe and B_o is the width of the pipe at the instant of transition. Upon reaching the instant of flow transition from orifice to weir, the remaining material above the top of the pipe and below the top of the dam is assumed to collapse and is transported along the breach channel at the current rate of sediment transport before further erosion occurs. The erosion then proceeds to cut a channel parallel to and along the remaining portion of the downstream face of the dam between the elevation of the bottom of the pipe and the bottom of the dam. The remaining erosion process is quite similar to that described for the overtopping type of failure with the breach channel now in a position similar to line A-A in Fig. 2.

The preceding general description of the erosion process was for a man-made dam. If a landslide dam is simulated, the process is identical except, due to the assumption that the landslide dam has no crest width (W_{cr}), the erosion initially commences with the breach channel in the position of line B-B in Fig. 2. A failure mode of overtopping or piping may be initiated for a landslide-formed dam.

Breach Width

The method of determining the width of the breach channel is a critical component of any breach model. In this model, the width of the breach is dynamically controlled by two mechanisms. The first assumes the breach has an initial rectangular shape as shown in Fig. 3. The width of the breach (B_o) is governed by the following relation:

$$B_o = B_r\, y \tag{11}$$

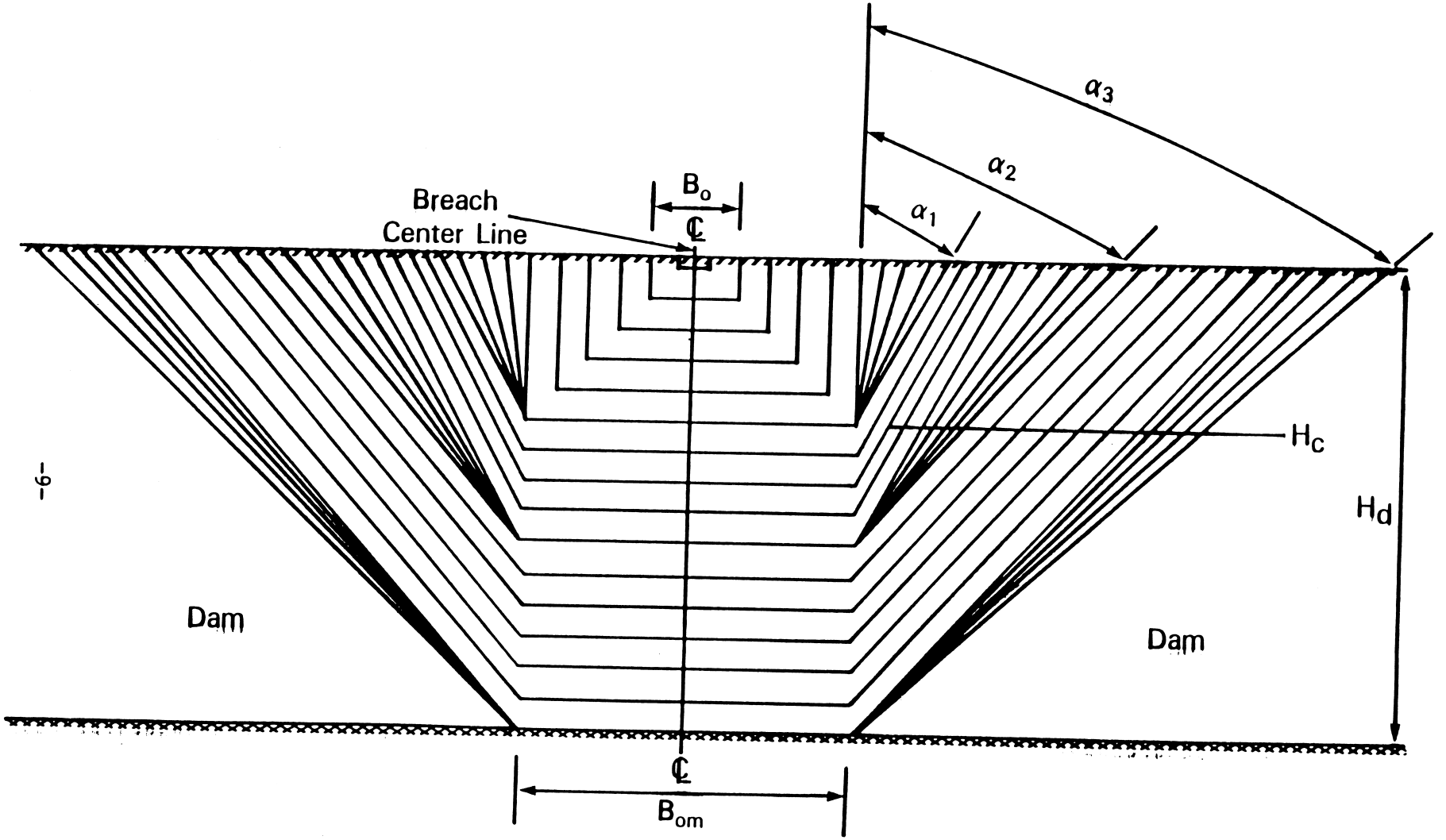

Figure 3. Front View of Dam with Breach Formation Sequence

in which B_r is a factor based on optimum channel hydraulic efficiency and y is the depth of flow in the breach channel. The parameter B_r has a value of 2 for overtopping failures while for piping failures, B_r is set to 1.0. The model assumes that y is the critical depth at the entrance to the breach channel, i.e.,

$$y = 2/3(H-H_c) \tag{12}$$

The second mechanism controlling the breach width is derived from the stability of soil slopes (Spangler, 1951). The initial rectangular-shaped channel changes to a trapezoidal channel when the sides of the breach channel collapse, forming an angle (α) with the vertical. The collapse occurs when the depth of the breach cut (H_c') reaches the critical depth (H') which is a function of the dam's material properties of internal friction (ϕ), cohesion (C), and unit weight (γ), i.e.,

$$H_k' = \frac{4\ C \cos\ \phi\ \sin\ \theta_{k-1}'}{\gamma\ [1\ -\ \cos\ (\theta_{k-1}'\ -\ \phi)]} \ldots\ k = 1,2,3 \tag{13}$$

in which the subscript k denotes one of three successive collapse conditions as shown in Fig. 3, and θ is the angle that the side of the breach channel makes with the horizontal as shown in Fig. 4. Thus, the angle (θ) or (α) at any time during the breach formation is given as follows:

$$\theta = \theta_{k-1}' \ldots\ldots\ldots H_k \leq H_k' \tag{14}$$

$$\theta = \theta_k' \ldots\ldots\ldots H_k > H_k' \tag{15}$$

$$B_o = B_r\ y. \ldots\ldots\ldots k = 1 \tag{16}$$

$$B_o = B_{om} \ldots\ldots\ldots k > 1 \tag{17}$$

$$B_{om} = B_r\ y \ldots\ldots\ldots \text{when } H_1 = H_1' \tag{18}$$

$$\alpha = 0.5\pi - \theta \tag{19}$$

where:

$$\theta_o' = 0.5\pi \tag{20}$$

$$\theta_k' = (\theta_{k-1}' + \phi)/2 \ldots\ldots k = 1,2,3 \tag{21}$$

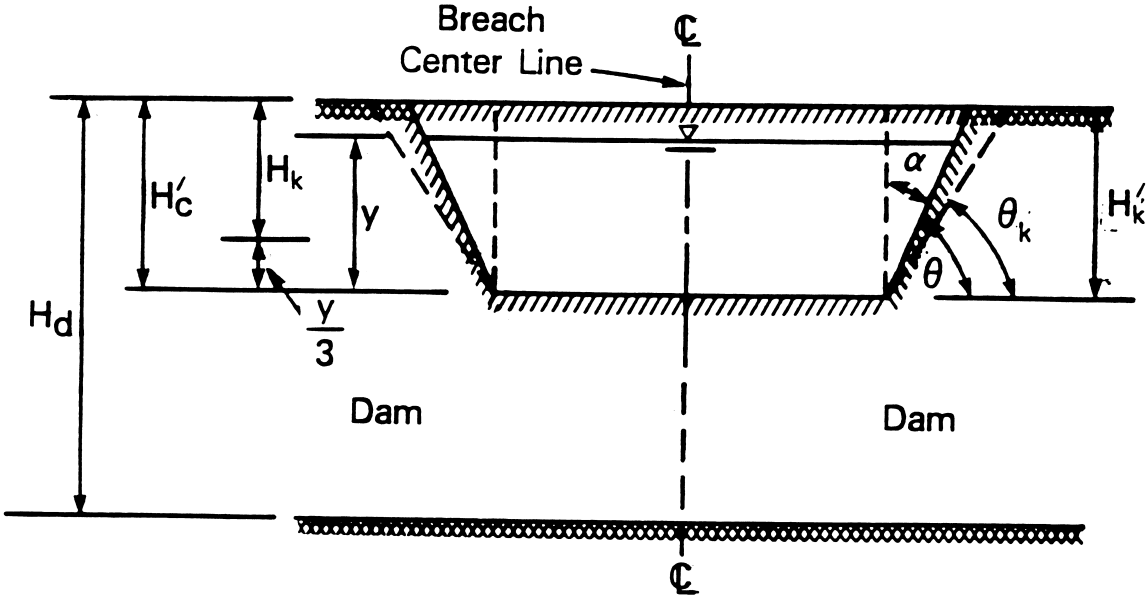

Figure 4. Front View of Dam with Breach

$$H_k = H_c' - y/3 \tag{22}$$

The subscript (k) is incremented by 1 at the instant when $H_k > H_k'$. In Eq. (22), the term (y/3) is subtracted from H_c' to give the actual free-standing depth of breach cut in which the supporting influence of the water on the stability of the sides of the breach is taken into account. Through this mechanism, it is possible for the breach to widen after the peak outflow through the breach has occurred since the flow depth (y) diminishes during the receding flow.

Erosion is assumed to occur equally along the bottom and sides of the breach channel except when the sides of the breach channel collapse. Thereupon, the breach bottom is assumed not to continue to erode downward until the volume of collapsed material along the breach is removed at the rate of the sediment transport capacity of the breach channel at the instant of collapse. After this characteristically short pause, the breach bottom and sides continue to erode.

When the breach has eroded downward to the original valley floor, further downward erosion is prohibited within the model; however, the sides of the breach continue to erode and the breach continues to widen. The occurrence of the outflow peak discharge may coincide with the breach bottom reaching the valley floor or at some time later as the breach sides continue to be eroded. The maximum discharge through the breach is dependent on the rate of breach enlargement via erosion and the rate at which the reservoir head decreases as a result of the increasing flow caused by the increasing breach opening. The model allows a maximum permissible breach bottom width and a maximum top width at the crest of the dam to be specified by the user; this approximately accounts for the original valley topography which is assumed to be nonerodible.

When landslide dams are simulated, the relatively long breach channel lengths, compared to those of man-made dams, suggest that the width for the channel be computed apart from the entrance width of the breach. In this case, y in Eqs. (11), (16), (18), and (22) is computed as the normal uniform depth (y_n) in the breach channel rather than the critical depth given by Eq. (12). Equations for computing the normal channel depth are presented in a subsequent section.

Reservoir Level Determination

Conservation of mass is used to compute the change in the reservoir water surface elevation (H) due to the influence of reservoir inflow (Q_i), spillway outflow (Q_{sp}), crest overflow (Q_o), breach outflow (Q_b), and the reservoir storage characteristics. The conservation of mass over a time step (Δt) in hours is represented by the following:

$$\bar{Q}_i - (\bar{Q}_b + \bar{Q}_{sp} + \bar{Q}_o) = S_a \frac{\Delta H \; 43560}{\Delta t \; 3600} \tag{23}$$

in which ΔH is the change in water surface elevation during the time interval (Δt), and S_a i the surface area in acres at elevation H. All flows are expressed in units of cfs, and the ba (-) indicates the flow is averaged over the time step. Rearranging Eq. (23) yields the following expression for the change in the reservoir water surface:

$$\Delta H = \frac{0.0826\ \Delta t}{S_a} (\bar{Q}_i - \bar{Q}_b - \bar{Q}_{sp} - \bar{Q}_o) \qquad (2$$

The reservoir elevation (H) at time (t) can easily be obtained from the relation,

$$H = H' + \Delta H \qquad (2$$

in which H' is the reservoir elevation at time $t-\Delta t$.

The reservoir inflow ($\bar{Q}_i$) is determined from the specified table of inflows (Q_i) vs. time (T_i). The spillway flow ($\bar{Q}_s$) is determined from the specified table of spillway flows (Q_s) vs. reservoir elevation (H). The breach flow (Q_b) is computed from Eq. (2) for piping flow. When the breach flow is weir-type, Eq. (1) is used when $H_c = H_u$; however, when H $< H_u$, the following broad-crested weir equation is used:

$$Q_b = 3\ B_o\ (H - H_c)^{1.5} + 2\ \tan(\alpha)\ (H - H_c)^{2.5} \qquad (2$$

in which B_o is given by Eq. (16) or Eq. (17) and α is given by Eq. (19). The crest overflo is computed as broad-crested weir flow from Eq. (1), where B_o is replaced by the crest length of the dam and H_c is replaced by H_u.

Breach Channel Hydraulics

The breach flow is assumed to be adequately described by quasi-steady uniform flow as determined by applying the Manning open channel flow equation at each Δt time step, i.e.,

$$Q_b = \frac{1.49\ S^{0.5}\ A^{1.67}}{n\qquad P^{0.67}} \qquad (2$$

in which $S = 1/ZD$, A is the channel cross-sectional area, P is the wetted perimeter of the channel, and n is the Manning coefficient. In this model, n is computed using the Strickler relation which is based on the average grain size of the material forming the breach channel, i.e.,

$$n = 0.013\ D_{50}^{0.167} \tag{28}$$

in which D_{50} represents the average grain size diameter expressed in mm.

The use of quasi-steady uniform flow is considered appropriate because the extremely short reach of breach channel, very steep channel slopes (1/ZD) for man-made dams, and even in the case of landslide dams where the channel length is greater and the slope is smaller, contribute to produce extremely small variation in flow with distance along the breach channel. The use of quasi-steady uniform flow in contrast to the unsteady flow equations as used by Ponce and Tsivoglou (1981) greatly simplifies the hydraulics and computational algorithm. Such simplification is considered commensurate with the other simplifications inherent in the treatment of the breach development in dams for which precise measurements of material properties are lacking or impossible to obtain and the wide variance which exists in such properties in many dams. The simplified hydraulics eliminates troublesome numerical computation problems and enables the breach model to require only minimal computational resources.

When the breach channel is rectangular, the following relations exist between depth of flow (y_n) and discharge (Q_b):

$$y_n = \left[\frac{Q_b\ n}{1.49\ B_o\ S^{0.5}} \right]^{0.6} \tag{29}$$

in which B_o is defined by Eqs. (16-18).

When the breach channel is trapezoidal, the following algorithm based on Newton-Raphson iteration is used to compute the depth of flow (y_n):

$$y_n^{k+1} = y_n^k - \frac{f\left(y_n^k\right)}{f'\left(y_n^k\right)} \tag{30}$$

$$f\left(y_n^k\right) = Q_b P^{0.67} - 1.49\ S^{0.5}\ A^{1.67} \tag{31}$$

in which

$$A = 0.5(B_o + B)\ y_n^k \tag{32}$$

$$B = B_{om} + y_n \tan(\alpha) \tag{33}$$

$$P = B_{om} + y_n/\cos(\alpha) \tag{34}$$

$$f'(y_n^k) = 0.67\ Q_b \frac{P'}{P^{1/3}} - 1.67 \frac{1.49}{n} S^{0.5}\ B\ A^{0.67} \quad (35)$$

in which

$$P' = 1/\cos(\alpha) \quad (36)$$

The superscript (k) is an iteration counter; the iteration continues until

$$|y_n^{k+1} - y_n^k| < \epsilon \qquad \epsilon \leq 0.01 \quad (37)$$

The first estimate for y_n is obtained from the following:

$$y_n^1 = \left[\frac{Q_b n}{1.49\ B\ S^{0.5}}\right]^{0.6} \quad (38)$$

where:

$$\bar{B} = 0.5(B_{cm} + B') \quad (39)$$

in which B' is the breach channel top width at the water depth (y_n) at ($t-\Delta t$).

Sediment Transport

The rate at which the breach is eroded depends on the capacity of the flowing water to transport the eroded material. The Meyer-Peter and Muller sediment transport relation as modified by Smart (1984) for steep channels is used, i.e.,

$$Q_s = 3.64\ (D_{90}/D_{30})^{0.2}\ P \frac{D^{2/3}}{n} S^{1.1}\ (DS - \Omega) \quad (40)$$

where:

$$\Omega = 0.0054\ \tau_c\ D_{50} \qquad \text{(noncohesive)} \quad (41)$$

$$\Omega = \frac{b'}{62.4}\ (PI)^{c'} \qquad \text{(cohesive)} \quad (42)$$

$$\tau_c = a'\ \tau_c' \quad (43)$$

$$a' = \cos\theta\ (1. - 1.54 \tan\theta) \quad (44)$$

$$\theta = \tan^{-1} S \quad (45)$$

$$\tau_c' = 0.122/R*^{0.970} \ldots\ R* < 3 \quad (46)$$

$$\tau_c' = 0.056/R*^{0.266} \ldots\ 3 \leq R* \leq 10 \quad (47)$$

$$\tau_c' = 0.0205\ R*^{0.173} \ldots\ R* > 10 \quad (48)$$

$$S = \frac{1}{ZD} \quad (49)$$

$$R* = 1524\ D_{50}\ (DS)^{0.5} \quad (50)$$

in which Q_s is the sediment transport rate (cfs); D_{30}, D_{50}, D_{90} (mm) are grain sizes at which 30, 50, and 90 percent of the total weight is finer; D is the hydraulic depth of flow (ft), S is the slope of the downstream face of the dam; and τ_c' is the Shields' dimensionless critical shear stress, PI is the plasticity index for cohesive soils, b' and c' are empirical coefficients with the following ranges: $0.003 \leq b' \leq 0.019$ and $0.58 \leq c' \leq 0.84$, respectively (Clapper and Chen, 1987).

Breach Enlargement By Sudden Collapse

It is possible for the breach to be enlarged by a rather sudden collapse failure of the upper portions of dam in the vicinity of the breach development. Such a collapse would consist of a wedge-shaped portion of the dam having a vertical dimension (Y_c) as shown in Fig. 5. The collapse would be due to the pressure of the water on the upstream face of the dam exceeding the resistive forces due to shear and cohesion which keep the wedge in place. When this occurs, the wedge is pushed to the right in Fig. 5 and is then transported by the escaping water through the now enlarged breach. When collapse occurs, the erosion of the breach ceases until the volume of the collapsed wedge is transported through the breach channel at the transport rate of the water escaping through the suddenly enlarged breach. A check for collapse is made at each Δt time step during the simulation. The collapse check consists of assuming an initial value for Y_c of 10 and then summing the forces acting on the wedge of height, Y_c. The forces are those due to the water pressure (F_w) and the resisting forces which are the shear force (F_{sb}) acting along the bottom of the wedge, the shear force (F_{ss}) acting along both sides of the wedge, the force (F_{cb}) due to cohesion along the wedge bottom and (F_{cs}), the force due to cohesion acting along the sides of the wedge. Thus, collapse occurs if:

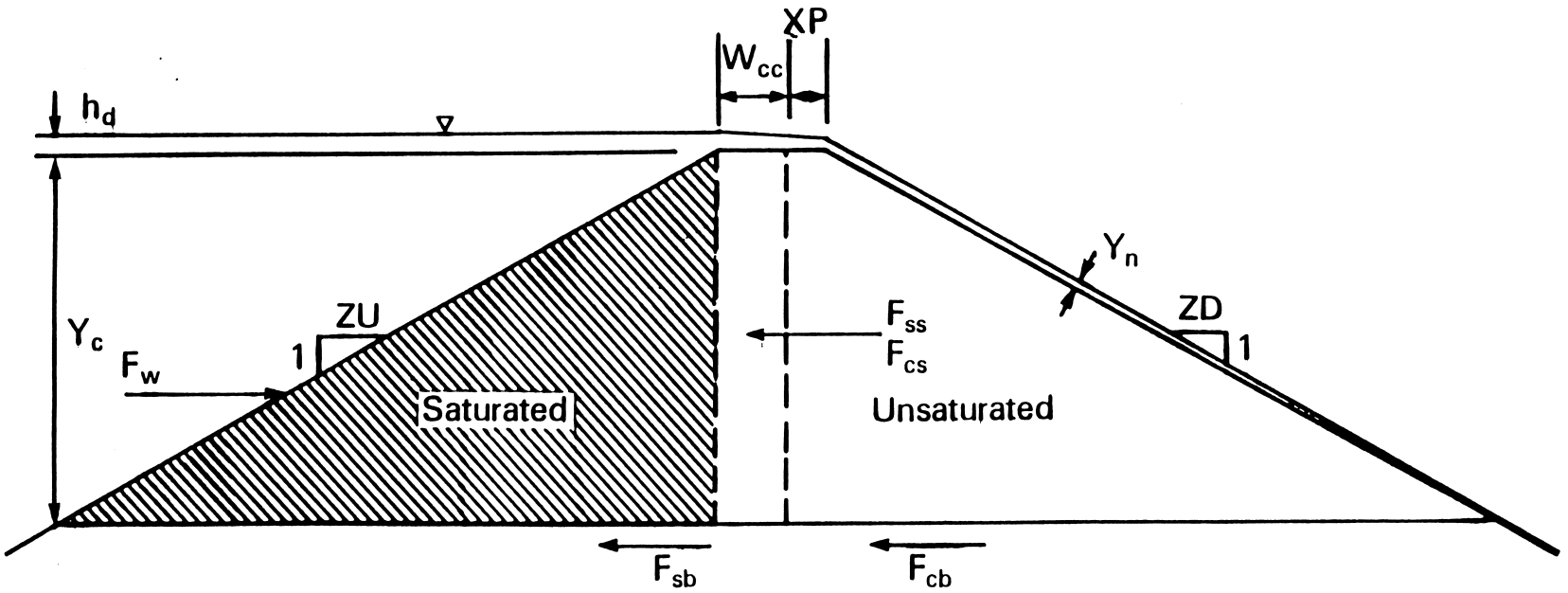

Figure 5. Side View of Dam Showing the Forces which Determine the Possible Collapse of the Upper Portion (Y_c) of the Dam

$$F_w > F_{sb} + F_{ss} + F_{cb} + F_{cs} \tag{51}$$

where:

$$F_w = 0.5\ 62.4\ \bar{B}\ (Y_c + 2\ h_d) \tag{52}$$

$$F_{sb} = \begin{array}{l} \tan\phi[(\gamma - 62.4)0.5\ ZU\ \bar{B}\ Y_c^2 + \gamma\ B\ W_{cc}\ Y_c + \\ \gamma\ 0.5\ ZD\ \bar{B}\ Y_c^2 + 0.67\ 62.4\ h_d\ W_{cc}\ B + 62.4\ ZD'\ B\ y_n\ Y_c] \end{array} \tag{53}$$

$$F_{ss} = \gamma K \tan\phi\ Y_c^2[W_{cc} + (ZU + ZD)Y_c] \tag{54}$$

$$F_{cb} = CB_o[W_{cc} + (ZU + ZD)\ Y_c] \tag{55}$$

$$F_{cs} = 2C[W_{cc} + (ZU + ZD)Y_c(B_o + 2Y_c/\cos\alpha)] \tag{56}$$

in which

$$K = (1 - \sin\phi)/(1 + \sin\phi) \tag{57}$$

$$\bar{B} = B_o + H_c \sin\alpha \tag{58}$$

$$ZD' = (1 + ZD^2)^{0.5} \tag{59}$$

and Y_c, h_d, ZU, ZD, W_{cc}, and y_n are defined in Fig. 5. The top width (B) of the water surface in the breach channel is defined by Eq. (11) or Eq. (33), and α is defined in Fig. 4 and Eq. (19).

If the inequality of Eq. (51) is not satisfied with the first trial Y_c, then no collapse occurs at this time. If it is satisfied, Y_c is increased by 2 ft and Eq. (51) is again evaluated. This cycle continues until the inequality is not satisfied. Then the final value for Y_c is assumed to be Y_c-1.

Computational Algorithm

The sequence of computations in the model are iterative since the flow into the breach is dependent on the bottom elevation of the breach and its width while the breach properties are dependent on the sediment transport capacity of the breach flow, and the transport capacity is dependent on the breach size and flow. A simple iterative algorithm is used to account for the mutual dependence of the flow, erosion, and breach properties. An estimated incremental erosion depth ($\Delta H_e'$) is used at each time step to start the iterative computation.

This estimated value can be extrapolated from previously computed incremental erosion depths after the first few time steps. The computational algorithm follows:

1. increment the time: $t = t' + \Delta t$;

2. compute H_c using estimated $\Delta H_c'$: $H_c = H_c' - \Delta H_c'$;

3. compute reservoir elevation: $H = H' + \Delta H$, where $\Delta H'$ is an estimated incremental change in the reservoir elevation as obtained by extrapolation from previous changes and H' is the reservoir elevation at time (t');

4. compute $\bar{Q}_{sp}$, $\bar{Q}_i$, $\bar{Q}_o$ associated with elevation H;

5. compute ΔH from Eq. (24) using the previously computed breach flow (Q_b);

6. compute reservoir elevation: $H = H' + \Delta H$;

7. compute breach flow (Q_b) using Eq. (1), Eq. (2), or Eq. (26);

8. correct breach flow for downstream submergence:

$$Q_b = S_b Q_b, \text{ where } S_b = 1.0 - 2.78 \left[\frac{Y_t - H_c}{H - H_c} - 0.67 \right]^3$$

in which y_t is the tailwater depth due to the total outflow ($Q_b + Q_{sp} + Q_o$), and is computed from the Manning equation applied to the tailwater cross-section;

9. compute B_o, α, B, P, and R for the breach channel using Eqs. (16-19) and (33-34);

10. compute sediment transport rate (Q_s) from Eq. (40);

11. compute ΔH_c as follows: $\Delta H_c = 3600\ \Delta t\ Q_s/[P_o\ L\ (1 - P_{or})]$ in which L is the length of the breach channel which may be easily computed from the geometric relations shown in Fig. 2, P_{or} is the porosity of the breach material, and P_o is the total perimeter of the breach, $P_o = B_o + 2(H_u - H_c)/\cos\alpha$;

12. compute ΔH_c with the estimated value $\Delta H_c'$: if $100\ (\Delta H_c' - \Delta H_c)/\Delta H_c < E$, where E is an error tolerance in percent (an

input to the model having a value between 0.1 and 1.0), then the solution for ΔH_c and the associated outflows Q_b, Q_s, and Q_o are considered acceptable; if the above inequality is not satisfied, step (2) is returned to with the recently computed ΔH_c replacing $\Delta H'_c$; this cycle is repeated until convergence is attained, usually within 1 or 2 iterations.

13. check for collapse;

14. extrapolate estimates for $\Delta H'_c$ and $\Delta H'$;

15. if t is less than the specified duration of the computation (t_c) return to step 1; and

16. plot the outflow hydrograph consisting of the total flow ($Q_b+Q_s+Q_o$) computed at each time step.

Computational Requirements

The basic time step (Δt) is specified; however, when rapid erosion takes place the basic time step is automatically reduced to $\Delta t/20$. The specified value for the basic time step is usually about 0.02 hrs with slightly larger values acceptable for landslide dams. For typical applications, the BREACH model requires less than 10 seconds of CPU time on a PRIME 750 computer and less than 2 seconds on an IBM 360/195 computer, both of which are main-frame computers. Although it has not been used on micro-computers, it would be quite amenable to such applications.

The model has displayed a lack of numerical instability or convergence problems. The computations show very little sensitivity to a reasonable variation in basic time step size. Numerical experimentation indicates that as the time step is increased by a factor of 4, the computed peak flow (Q_p), time of peak (T_p), and final breach dimensions vary by less than 10, 4, and 0.5 percent, respectively.

Comparison With Previous Models

The BREACH model differs from the models of Cristofano (1965) and Harris and Wagner (1967) in the following significant ways:

1) the sediment transport algorithm utilized;

2) the method used for changing the breach shape and width;

3) the delay in breach erosion downward until the downstream face has been sufficiently eroded;

4) the introduction of a possible collapse mechanism for breach enlargement;

5) the accommodation of a piping failure mode; and

6) the consideration of possible tailwater submergence effects on the breach flow.

Similarities are their simplicity of the computational algorithm, the use of the D_{50} grain size and internal friction angle (ϕ) and the assumption of quasi-steady uniform flow hydraulics.

The BREACH model differs from the model reported by Ponce and Tsivoglou (1981) in the following significant ways:

1) items 1, 2, 4, 5, and 6 as stated above;

2) the much simpler computational algorithm used in BREACH;

3) the use of the internal friction angle;

4) the use of the D_{50} grain size for determining the Manning n; and

5) consideration of spillway flows for man-made dams.

Similarities between the two models include the gradual development of the breach channel along the downstream face of the dam prior to its erosion vertically through the dam's crest, the use of the Manning n for the breach channel hydraulics, and the way in which the reservoir hydraulics are included in the development of the breach.

MODEL APPLICATIONS

The BREACH model was applied to four earthen dams to determine the outflow hydrograph produced by a gradual breach of each. The first was an actual piping failure of the man-made Teton Dam in Idaho, the second was an actual piping failure of the man-made Lawn Lake Dam in Colorado, the third was an actual overtopping failure of the landslide-formed dam which blocked the Mantaro River in Peru, and the fourth was a hypothetical piping failure of the landslide dam which blocks the natural outlet of Spirit Lake near Mount St. Helens in Washington.

Teton Dam

The Teton Dam, a 300 ft high earthen dam with a 3000 ft long crest and 262 ft depth of stored water amounting to about 250,000 acre-ft, failed on June 5, 1976. According to a report by Ray, et al. (1976), the failure started as a piping failure about 10:00 am and slowly increased the rate of outflow until about 12:00 noon when the portion of the dam above the

piping hole collapsed and in the next few minutes (about 12 minutes according to Blanton (1977)) the breach became fully developed allowing an estimated 1.6 to 2.8 million cfs (best estimate of 2.3) peak flow (Brown and Rogers, 1977) to be discharged into the valley below. At the time of peak flow the breach was estimated from photographs to be a trapezoidal shape having a top width at the original water surface elevation of about 500 ft and side slopes of about 1 vertical to 0.5 horizontal. After the peak outflow, the outflow gradually decreased to a comparatively low flow in about 5 hours as the reservoir volume was depleted and the surface elevation receded. The downstream face of the dam had a slope of 1:2 and the upstream face 1:2.5. The crest width was 35 ft and the bulk of the breach material was a D_{50} size of 0.03 mm. The inflow to the reservoir during failure was insignificant and the reservoir surface area at time of failure was about 1950 acre-ft.

The BREACH model was applied to the piping generated failure of the Teton Dam. The centerline elevation for the piping breach was 160 ft above the bottom of the dam, and an initial width of 0.1 ft was used for the assumed square-shaped pipe. The material properties of the breach were assumed as follows: ϕ = 40 deg, C = 250 lb/ft^2, and γ = 100 lb/ft^3. The Strickler equation was judged not to be applicable for the extremely fine breach material, and the n value was computed as 0.013 from a Darcy friction factor based on the D_{50} grain size and the Moody curves (Morris and Wiggert, 1972). The computed outflow hydrograph is shown in Fig. 6. The timing, shape, and magnitude of the hydrograph compares quite well with the estimated actual values. The computed peak outflow of 2.3 million cfs agrees with the best estimate made by the U.S. Geological Survey, and the time of occurrence is also the same. The computed breach width of 571 ft at the time of peak overflow agrees with the estimated value of about 500 ft at the elevation of the initial reservoir water surface. A larger estimated actual breach width of 650 ft was reported by Brown and Rogers (1977); however, this was the final breach width after additional enlargement of the breach occurred. The (BREACH) model produced a final width of 630 ft when the reservoir water elevation had receded to near the reservoir bottom; the additional widening of the breach during the recession of the outflow is due to continued erosion of the sides and the influence of the depth (y) in Eq. (15).

Sensitivities of the peak breach outflow (Q_p), time of peak flow (T_p), and the top width (W) of the trapezoidal-shaped breach to variations in the specified breach material properties, cohesive strength (C), and internal friction angle (ϕ) are shown in Fig. 7. The dashed lines apply to the Teton simulation. Peak outflow is moderately affected by the cohesion; however, it is sensitive to the ϕ value which mostly controls the enlargement of the breach width. Q_p is sensitive to a full range of ϕ values; however, the ϕ value may vary by $\pm$10 degrees with less than 20 percent variation in Q_p. The breach width (W) was moderately sensitive to variations in the cohesion (C), and somewhat more sensitive to the ϕ value. The time to peak outflow (T_p) was almost insensitive to variations in C and ϕ.

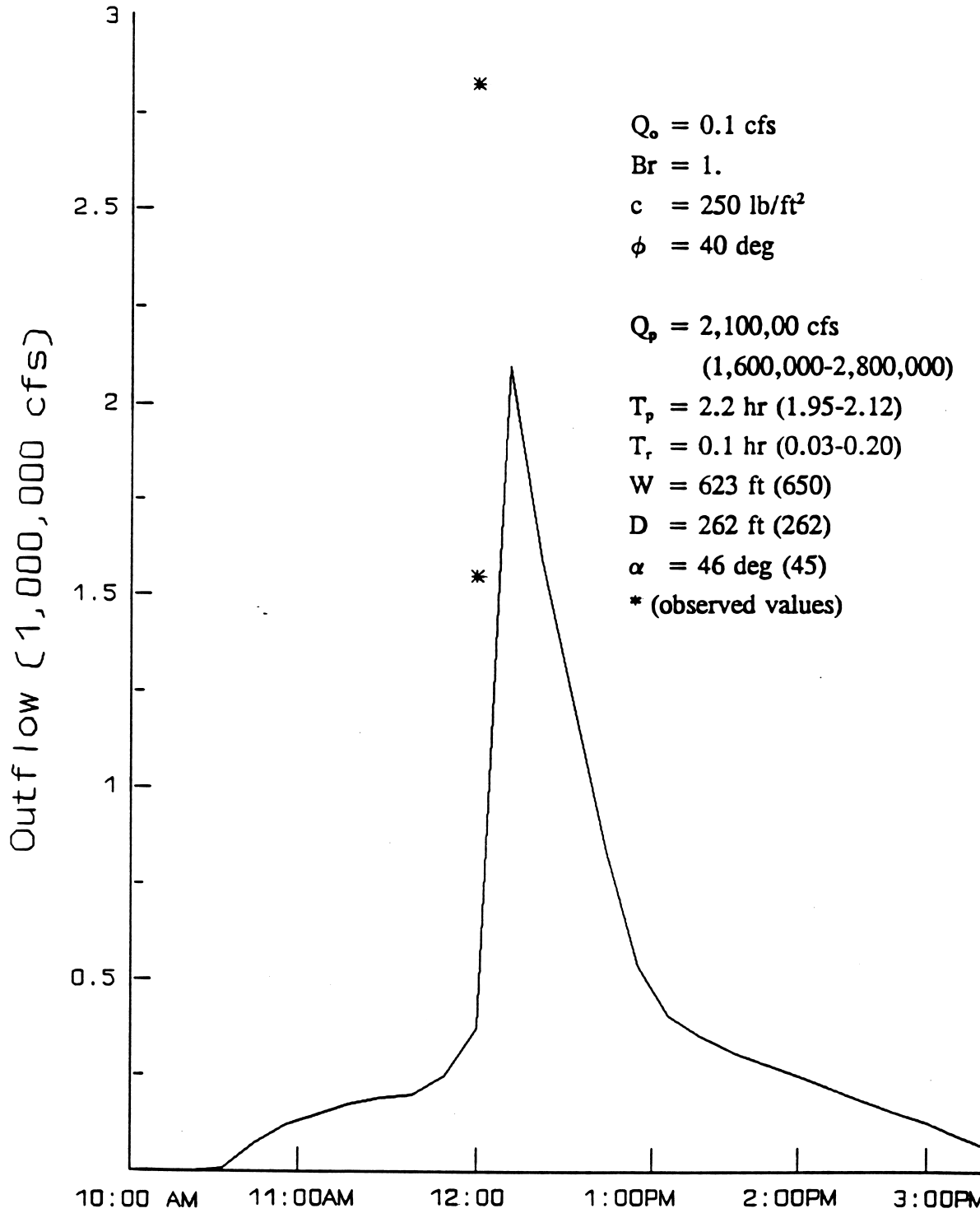

Figure 6. Teton Dam: Predicted and Observed Breach Outflow Hydrograph and Breach Properties

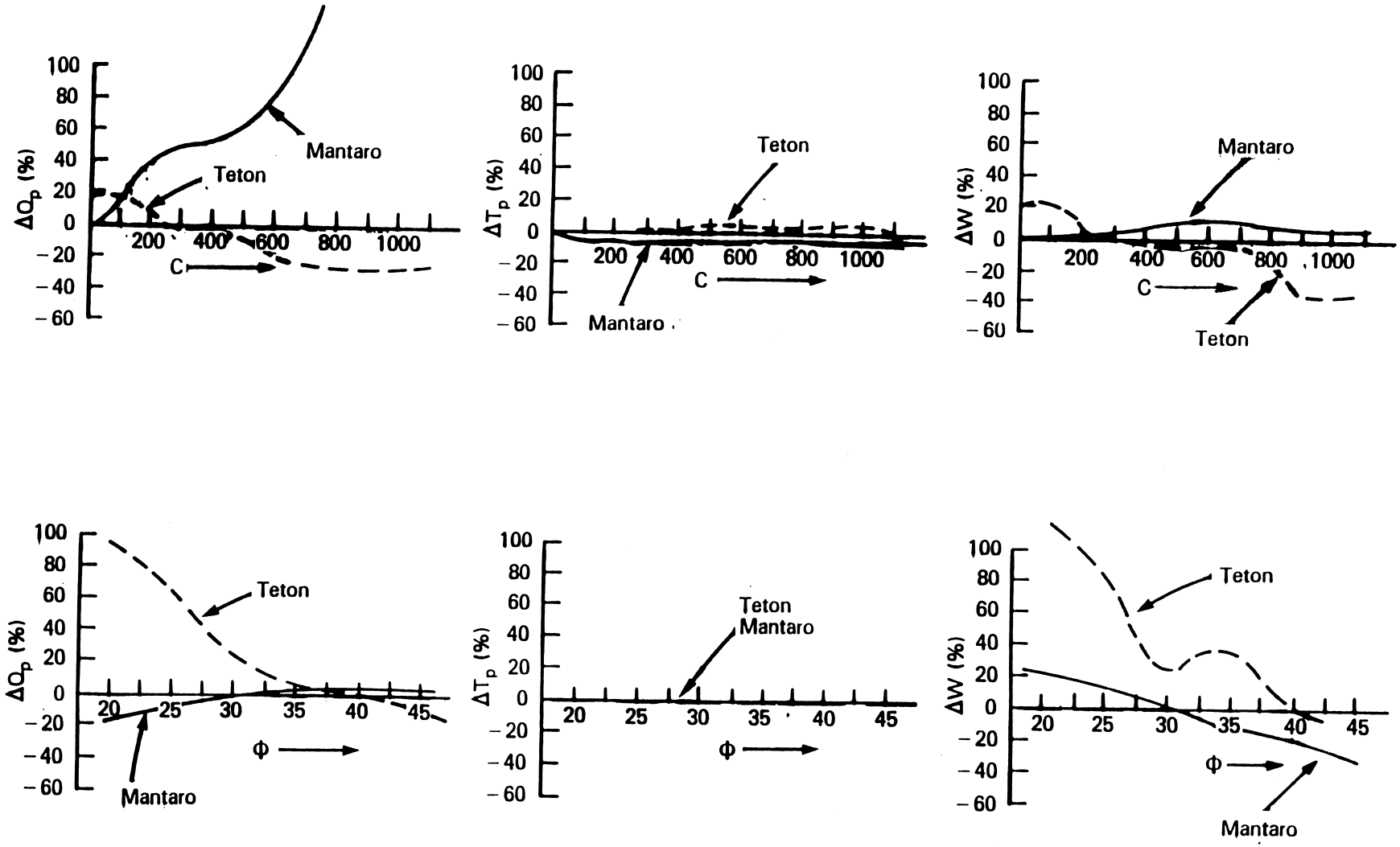

Figure 7. Sensitivity of Mantaro and Teton Predictions of Peak Outflow (Q_p), Time to Peak (T_p), and Breach Width (W) to Changes in the Material Properties of the Dam: Cohesion (C) and Internal Friction Angle (ϕ)

Lawn Lake Dam

The Lawn Lake Dam, a 26 ft high earthen dam with approximately 800 acre-ft of storage, failed July 15, 1982, by piping along a bottom drain pipe (Jarrett and Costa, 1984). The BREACH model was applied with the piping breach assumed to commence within 2 ft of the bottom of the dam. The material properties of the breach were assumed as follows: D_{50} = 0.25 mm, ϕ = 25 deg, C = 100 lb/ft^2, and γ = 100 lb/ft^3. The downstream face of the dam had a slope of 1:1.3 and the upstream face 1:1.5. The computed outflow was 17,925 cfs, while the estimated actual outflow was 18,000 cfs. The model produced a trapezoidal-shaped breach with top and bottom dimensions of 132 and 68 ft, respectively. The actual breach dimensions were 97 and 55 ft, respectively. The mean observed breach width was about 32 percent smaller than the mean breach width produced by the model.

Mantaro Landslide Dam

A massive landslide occurred in the valley of the Mantaro River in the mountainous area of central Peru on April 25, 1974. The slide, with a volume of approximately 5.6 x 10^{10}ft^3, dammed the Mantaro River and formed a lake which reached a depth of about 560 ft before overtopping during the period June 6-8, 1974 (Lee and Duncan, 1975). The overtopping flow very gradually eroded a small channel along the approximately 1 mile long downstream face of the slide during the first 2 days of overtopping. Then a dramatic increase in the breach channel occurred during the next 6-10 hrs resulting in a final trapezoidal-shaped breach channel approximately 350 ft in depth, a top width of some 800 ft, and side slopes of about 1:1. The peak flow was estimated at 353,000 cfs as reported by Lee and Duncan (1975), although Ponce and Tsivoglou (1981) later reported an estimated value of 484,000 cfs. The breach did not erode down to the original river bed; this caused a rather large lake to remain after the breaching had subsided some 24 hrs after the peak had occurred. The slide material was mostly a mixture of silty sand with some clay resulting in a D_{50} size of about 11 mm with some material ranging in size up to 3 ft boulders.

The BREACH model was applied to the Mantaro landslide-formed dam using the following parameters: ZU = 17, ZD = 8.0, H_u = 560 ft, D_{50} = 11 mm, P_{or} = 0.55, S_a = 1200 acres, C = 30 lb/ft^2, ϕ = 38 deg, γ = 100 lb/ft^3, B_r = 2, and Δt = 0.1 hr. The Manning n was estimated by Eq. (28) as 0.020 and the initial breach depth was assumed to be 0.035 ft. The computed breach outflow is shown in Fig. 8 along with the estimated actual values. The timing of the peak outflow and its magnitude are very similar. The dimensions of the gorge eroded through the dam are similar as shown by the values of D, W, and α in Fig. 8.

The sensitivities of Q_p, T_p, and W for variations in C and ϕ are shown in Fig. 7. The solid line denotes the Mantaro application. Most notably, Q_p is very sensitive to the cohesion (C) while much less sensitive to the internal friction angle (ϕ). T_p is almost insensitive to the value of C and quite insensitive to ϕ. W is not very sensitive to C and

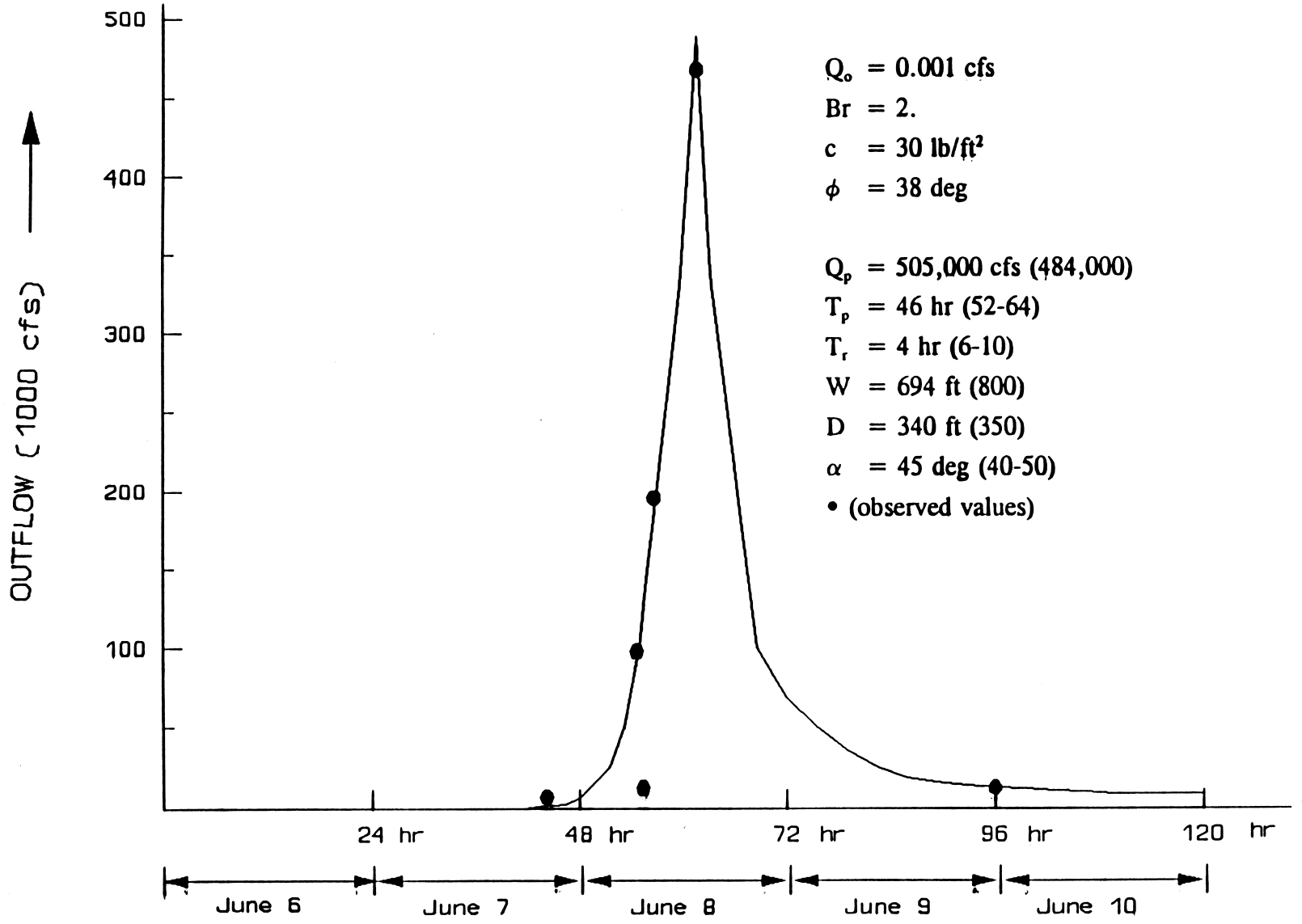

Figure 8. Mantaro Landslide Dam: Predicted and Observed Breach Outflow Hydrograph and Breach Properties

moderately sensitive to ϕ; a variation of ± 10 degrees in ϕ results in a change in W of less than 20 percent.

Spirit Lake Blockage

The violent eruption of Mount St. Helens on May 18, 1980, in Washington, produced a massive debris avalanche which moved down the north side of the volcano depositing about 105 billion ft^3 of materials in the upper 17 miles of the North Fork of the Toutle River valley and blocking the former outlet channel of Spirit Lake with deposits of up to 500 ft deep (Swift and Kresch, 1983). Spirit Lake itself was drastically changed by the avalanche; the existing lake has a maximum volume of 314,000 acre-ft at the elevation of 3475 msl when breaching of the debris blockage is anticipated. To avoid this, the Corps of Engineers have installed temporary pumps to maintain the lake level at about elevation 3462 (275,000 acre-ft) and are expecting to complete in the near future a permanent outlet channel which will bypass the debris dam and maintain safe lake levels.

Greater than normal precipitation, failure of the pumping system, and/or addition of more avalanche material from another eruption of the volcano could cause the lake level to exceed elevation 3475 and possibly cause the debris dam to fail. Such a hypothetical breach was simulated using the BREACH model.

An initial piping failure was assumed to occur at elevation 3448. The following parameters were determined from physical considerations:

$H_u = 3475$, $H_p = 3448$, $H_f = 3320$, $ZD = 30$, $ZU = 22$, $D_{50} = 7$,
$n = 0.018$ (from Eq. (28)), $P_{or} = 0.32$, $\gamma = 100$, $\phi = 35$, $C = 150$,
$B_r = 1$, an initial pipe width of 0.1 ft, and $\Delta t = 0.20$ hr.

The simulated outflow hydrograph shown in Fig. 9 has a peak of about 550,000 cfs occurring 15 hrs after the start of failure. The time of rise (T_r) is about 2 hrs. The final breach dimensions are: $D = 155$ ft, $W = 420$ ft, and $\alpha = 50$ deg. Sensitivity tests indicate about a 20 percent variation in the peak flow may occur with expected variation in the internal friction angle and cohesion values. The predicted outflow hydrograph from Spirit Lake was used in a hazard investigation of possible mud flows along the Toutle and Cowlitz Rivers by Swift and Kresch (1983).

SUMMARY

A breach erosion model (BREACH) based on principles of hydraulics, sediment transport, and soil mechanics is described. The model uses equations of weir or orifice flow to simulate the outflow entering a channel that is gradually eroded through an earthen man-made or landslide-formed dam. Conservation of reservoir inflow, storage volume, and outflow (crest overflow, spillway flow, and breach flow) determines the time-dependent reservoir water elevation which, along with the predicted breach bottom elevation, determines the head controlling the reservoir outflow. A sediment transport relation, the

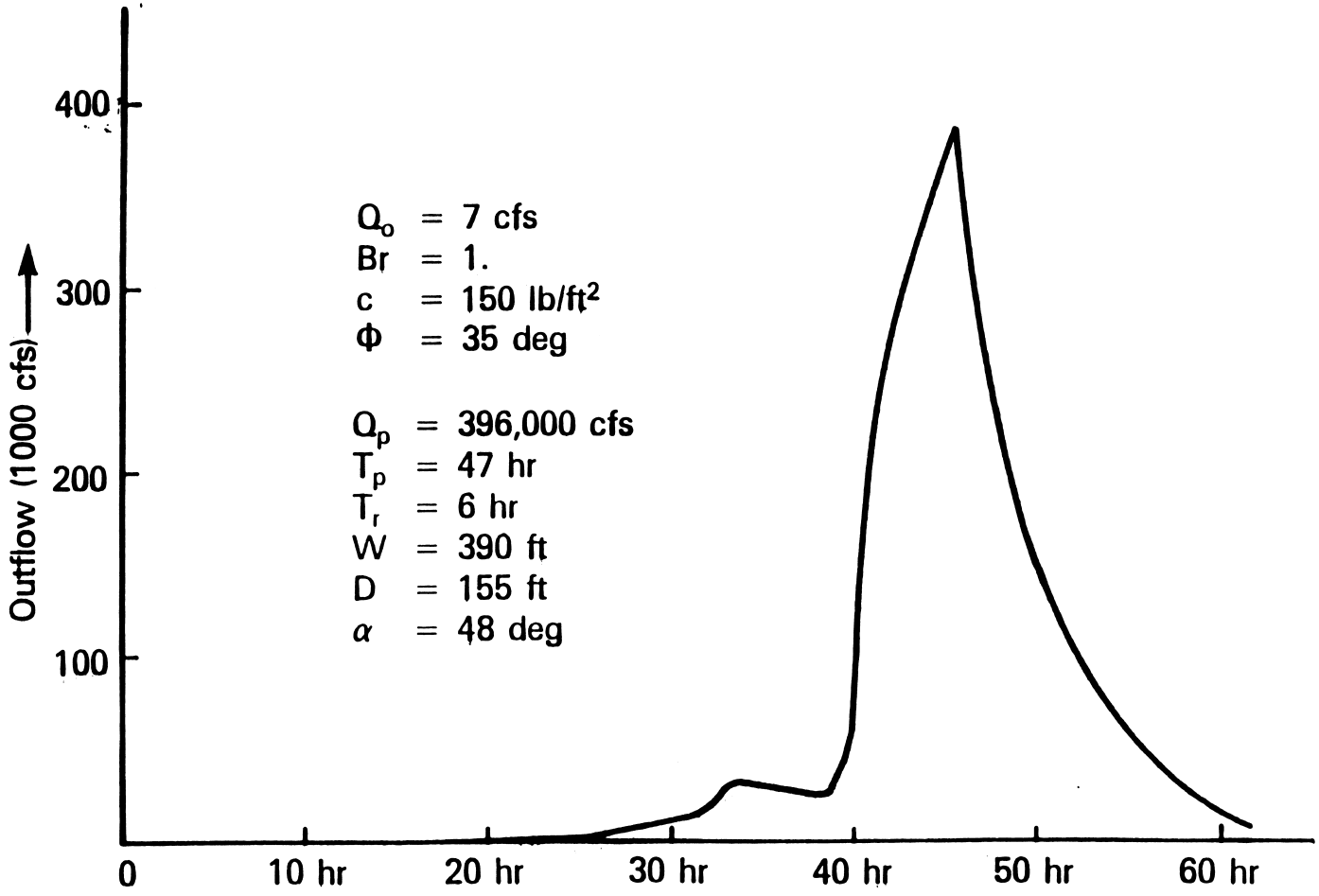

Figure 9. Spirit Lake Landslide Dam: Predicted Breach Outflow Hydrograph

Meyer-Peter and Muller equation modified for steep channels, is used to predict the transport capacity of the breach flow whose depth is determined by a quasi-steady uniform flow relation (the Manning equation applied at each Δt time step during the breach simulation). Breach enlargement is governed by the rate of erosion which is a function of the breach bottom slope and depth of flow and by the extent of collapse that occurs to the sides of the breach due to one or more sequential slope failures. The breach material properties (internal friction angle (ϕ) and cohesive strength (C)) are critical in determining the extent of enlargement of the trapezoidal-shaped breach. The Manning n used to compute the flow depth in the breach channel may be predicted on the basis of the grain size of the breach material by the Strickler equation or via the Moody relations. The dam may consist of three different materials: an inner core, an outer portion of the dam, and a thin layer along the downstream face of the dam. The latter is grass covered or of a grain size substantially larger than that of the outer portion of the dam. Piping or overtopping failure modes can be simulated, as well as sudden collapses of sections of the breach due to excessive hydrostatic pressure. The model has the potential to determine if a breach will develop sufficiently during an overtopping of the dam to cause a catastrophic release of the reservoir's stored water. The BREACH model has a simple iterative computational structure which has well-behaved and efficient numerical properties. A few seconds of computer time is required for a typical application.

The model is tested on a man-made dam (Teton Dam) which failed by an initial piping which progressed to a weir type free surface breach. The predicted outflow hydrograph and breach size and shape compare favorably with estimated actual values. The predictions are somewhat sensitive to the value of the internal friction angle (ϕ) which was estimated from a grain size and qualitative description of the dam's material composition.

The model is tested on a man-made dam (Lawn Lake) which failed by piping. The predicted outflow hydrograph and breach size and shape compare favorably with estimated actual values.

The model is also tested on the naturally formed landslide blockage of the Mantaro River in Peru which was overtopped and developed a large gorge which resulted in the gradual release of three-fourths of its stored water. The model predictions compared well with estimated observed values. The cohesive strength (C) is critical to the prediction of the rate of outflow of massive landslide dams; however, if it is selected on the basis of the breach material's properties, the results are within a reasonable range of variation.

It is considered that further testing of the model to assess its ability to predict overtopping failures of man-made dams is warranted and that its basic structure is suited to the resources (data and computational) which are commonly available to hydrologists/engineers during a detailed investigation of potential dam-failure flooding.

REFERENCES

Blanton, J.O. III. 1977. Flood plain inundation caused by dam failure. Proceedings of the Dam-Break Flood Routing Workshop. Water Resources Council, 47-64.

Brown, R.J., and D.C. Rogers. 1977. A simulation of the hydraulic events during and following the Teton Dam failure. Proceedings of the Dam-Break Flood Routing Workshop. Water Resources Council, 131-163.

Chow, V.T. 1959. Open-channel Hydraulics, McGraw-Hill Book Co., New York, 179-188.

Clapper, P.E., and Y.H. Chen. 1987. Predicting and minimizing embankment damage due to flood overtopping. Hydraulic Engineering. Proceedings of 1987 National Conference on Hydraulic Engineering. Ed. R. Ragan, 751-757.

Cristofano, E.A. 1965. Method of computing erosion rate for failure of earthfill dams. United States Bureau of Reclamation, Denver, Colorado.

Fread, D.L. 1977. The development and testing of a dam-break flood forecasting model. Proceedings of the Dam-Break Flood Routing Workshop. Water Resources Council, 164-197.

Fread, D.L. 1980. Capabilities of NWS model to forecast flash floods caused by dam failures. Proceedings of the Second Conference on Flash Floods. American Meteorological Society, 171-178.

Fread, D.L. 1982. DAMBRK: The NWS dam-break flood forecasting model. Hydrologic Research Laboratory, National Weather Service, Silver Spring, Maryland, 56 pp.

Fread, D.L. 1984. A breach erosion model for earthen dams. Proceedings of the Specialty Conference on "Delineation of Landslide, Flash Flood, and Debris Flow Hazards in Utah," Utah State University, Logan, Utah, 30 pp.

Harris, G.W., and D.A. Wagner. 1967. Outflow from breached earth dams. University of Utah, Salt Lake City, Utah.

Jarrett, R.D., and J.E. Costa. 1984. Hydrology, geomorphology, and dam-break modeling of the July 15, 1982, Lawn Lake Dam and Cascade Lake Dam failures, Larimer County, Colorado. Open File Report 84-162, U.S. Geological Survey, 107 pp.

Lee, K.L., and J.M. Duncan. 1975. Landslide of April 25, 1974 on the Mantaro River, Peru. National Academy of Sciences, Washington, D.C., 72 pp.

Morris, H.M., and J.M. Wiggert. 1972. Applied Hydraulics in Engineering. The Ronald Press Co., New York, 69-70, 290, 451-452, 460.

Ponce, V.M., and A.J. Tsivoglou. 1981. Modeling of gradual dam-breaches, Journal of Hydraulics Division, American Society of Civil Engineers, 107(HY6):829-838.

Ray, H.A., L.C. Kjelstrom, E.G. Crosthwaite, and W.H. Low. 1976. The flood in southeastern Idaho from Teton Dam failure of June 5, 1976. Open File Report, U.S. Geological Survey, Boise, Idaho.

Smart, G.M. 1984. Sediment transport formula for Steep Channels. Journal of Hydraulics Division, American Society of Civil Engineers, 110(HY3):267-276.

Spangler, M.G. 1951. Soil Engineering. International Textbook Co., Scranton, Pennsylvania, 321-323.

Swift, C.H. III, and D.L. Kresch. 1983. Mudflow hazards along the Toutle and Cowlitz Rivers from a hypothetical failure of Spirit Lake blockage. Water-Resources Investigations Report 82-4125, U.S. Geological Survey, Tacoma, Washington, 10 pp.

APPENDIX A

INPUT DATA FOR BREACH EROSION MODEL (BREACH): VERSION 7/88-1

Card No. — Data Description and Input Form

(1) MESSAGE - 20A4

MESSAGE	Any message such as name of dam, message may be $\leq$ 80 characters.

(2) HI, HU, HL, HPI, HSP, PI, CA, CB - 5F10.2

HI	Initial elevation (ft) of water surface in reservoir at t = 0.
HU	Elevation of top of dam.
HL	Elevation of bottom of dam (usually original stream-bed elevation).
HPI	Elevation at which piping failure commences (if no piping failure is simulated, leave blank).
HSP	Elevation of spillway crest (if no spillway, leave blank).
PI	Average plasticity index for clay of predominately clay dams.
CA	Coefficient (τ_c = CA (PI) ** CB) for clay critical shear stress, 0.004 < CA < 0.02.
CB	Coefficient (τ_c = CA (PI) ** CB) for clay critical shear stress, 0.58 < CB < 0.84.

(3) QIN(I) - 8F10.2

QIN(I)	Inflow (cfs) to reservoir. I subscript goes from 1 to 8. Inflow hydrograph may be defined with from 2 to 8 values.

(4) TIN(I) - 8F10.2

TIN(I)	Time (hrs) associated with QIN(I) reservoir inflow.

Card
No. Data Description and Input Form

(5) RSA(I) - 8F10.2

RSA(I) Surface area (acres) of reservoir. I subscript goes from 1 to 8. Surface area is defined at from 2 to 8 elevations starting at the highest elevation and proceeding to the reservoir bottom.

(6) HSA(I) - 8F10.2

HSA(I) Elevation (ft) associated with RSA(I) surface area.

(7) HSTW(I) - 8F10.2

HSTW(I) Elevation associated with top widths of tailwater cross-section. Elevations start at invert. I goes from 1 to maximum of 8.

(8) BSTW(I) - 8F10.2

BSTW(I) Top widths of tailwater cross-section.

(9) CMTW(I) - 8F10.3

CMTW(I) Manning's n associated with each top width of the tailwater cross-section.

(10) ZU, ZD, ZC, GL, GS, VMP, SEDCON - 7F10.2

ZU Slope of upstream face of dam [1 (vertical) : ZU (horizontal)].
ZD Slope of downstream face of dam [(1 (vertical) : ZD (horizontal)].
ZC Average slope of upstream and downstream faces of inner core of dam [1 (vertical) : ZC (horizontal)]. If no inner core, leave blank.
GL Average length of grass (inches). If no grass, leave blank.
GS Condition of stand of grass. If good, GS = 1.0; if poor stand or no grass exists, GS = 0.0.

Card
No. Data Description and Input Form

VMP	Maximum permissible velocity (ft/sec) for grass-lined channel before grass cover is eroded away. Can vary from 3 to 6 ft/sec. If no grass, leave blank.
SEDCON	Maximum sediment concentration (0.4 to 0.5) in breach flow. If left blank, default value of 0.5 is used.

(11) D50C, PORC, UWC, CNC, AFRC, COHC, UNFCC - 3F10.2, F10.4, 3F10.2

D50C	D50 (mm) grain size of inner core material (50 percent finer). If no core, leave blank.
PORC	Porosity ratio of inner core material. If no core, leave blank.
UWC	Unit weight (lb/ft^3) of inner core material. If no core, leave blank.
CNC	Manning n of inner core material. If left blank, it will be computed from the Strickler Equation which is a function of the grain size. If a value greater than 0.99 is entered, it will be computed from a Moody diagram (Darcy f vs. D50 relationship). If no core, leave blank.
AFRC	Internal friction angle (degree) of inner core material. If no core, leave blank.
COHC	Cohesive strength (lb/ft^2) of inner core material. If no core, leave blank.
UNFCC	Ratio of D90 to D30 grain sizes of inner core material. If no core, leave blank. If core exists and left blank, default value is 10.

(12) D50S, PORS, UWS, CNS, AFRS, COHS, UNFCS - 3F10.2, F10.4, 3F10.2

D50S	D50(mm) of outer material of dam (50 percent finer).
PORS	Porosity ratio of outer material.
UWS	Unit weight (lb/ft^3) of outer material.
CNS	Manning n of outer material. If left blank, it will be computed from the Strickler Equation which is a function of the grain size. If a value greater than 0.99 is entered, it will be computed from a Moody diagram (Darcy f vs. D50 relationship).
AFRS	Internal friction angle (degree) of outer material.
COHS	Cohesive strength (lb/ft^2) of outer material.

Card
No. Data Description and Input Form

UNFCS	Ratio of D90 to D30 grain size of outer material. If left blank, default value is 10.

Note: If dam material is homogeneous, use the outer layer to represent the entire homogenous dam material.

(13) BR, WC, CRL, SM, D50DF, UNFCDF, BMX, BTMX - 4F10.2, F10.4, 3F10.2

BR	Ratio of breach width to flow depth for initial rectangular-shaped breach. Range of values are: $1 \leq B \leq 2$. Usually use 2.0 for overtopping failure and 1.0 for a piping failure. If left blank, BR = 2.
WC	Width (ft) of crest of dam (can be zero).
CRL	Length (ft) of crest of dam.
SM	Bottom slope (ft/mile) of downstream river for first few thousand feet below the dam.
D50DF	D50 (mm) grain size of material composing the top one-foot of the downstream face of the dam. If left blank, D50DF = D50S.
UNFCDF	Ratio of D90 to D30 grain size of material of downstream face. If left blank, UNFCDF = 3.0 when D50DF > 0.0, or UNFCDF = UNFCS when D50DF = 0.0.
BMX	Maximum allowable width (ft) of breach bottom as restrained by valley cross-section (default to CRL in card 13).
BTMX	Maximum allowable width (ft) of breach top as restrained by valley cross-section (default to CRL in card 13).

(14) DTH, DBG, H, TEH, ERR, FPT, TPR - 2F10.3, 5F10.2

DTH	Basic time step size (hr). $0.001 \leq$ DTH ≤ 0.20, lower values for man-made dams, larger values for large landslide dams. If left blank, DTH = 0.005.
DBG	Output control parameter. DBG = 0.0, minimal output of discharge hydrograph only. DBG = 0.001, output at each time step + hydrograph. DBG = 0.002, output at each iteration of each time step + hydrograph.

Card
No. Data Description and Input Form

H	Initial depth (ft) of breach along the downstream face of dam for overtopping failure. Initial width of piping breach. Usually, $0.1 \leq H \leq 1.0$. If left blank, H = 0.10. Must be sufficiently large to cause some degree of initial breach enlargement.
TEH	Duration (hrs) of simulation.
ERR	Error tolerance in iterative solution, expressed as a percentage ratio ($0.1 \leq ERR \leq 1.0$). If left blank, ERR = 0.5.
FPT	Interval of time steps at which computed discharges are plotted ($1. \leq FPT \leq 10.$). If left blank, FPT = 10.0.
TPR	Output for DBG $\geq$ 0.0001 at time step is suppressed until time = TPR. If left blank, output is printed for all time steps.

Note: Omit cards no. (15) and (16) if spillway crest elev., HSP, (card no. 2) is blank or zero.

(15) SPQ(I) - 8F10.2

SPQ(I)	Spillway flow (cfs). I subscript goes from 1 to 8. Spillway flow is defined for from 2 to 8 heads starting at the spillway crest elev. and proceeding upwards until maximum spillway discharge is specified.

(16) SPH(I) - 8F10.2

SPH(I)	Head (ft) associated with SPQ(I) spillway flow.

OUTPUT PARAMETERS FOR "BREACH" MODEL, VERSION 7/88-1

I	COUNTER
T	TIME,HR
DTH	TIME STEP,HR
KG	CODE FOR REGION OF FAILURE : - 1 RESERVOIR FILLING
	0 NO EROSION ON GRASS
	1 EROSION OF DOWNSTREAM FACE
	2 EROSION OF UPSTREAM FACE
	3 DRAINING OF RESERVOIR WITH BREACH SIZE FIXED AT MAX DIMENSIONS
	4 PIPING MODE
	5 COLLAPSE MODE
KC	COLLAPSE HEIGHT
QTOT	TOTAL OUTFLOW, CFS
QTS	SPILLWAY OUTFLOW, CFS
QB	BREACH OUTFLOW, CFS
SUB	SUBMERGENCE CORRECTION FACTOR
BT	TOP WIDTH OF BREACH, FT
HY	ELEV OF RESERVOIR WATER SURFACE, FT
HC	ELEV OF BOTTOM OF BREACH, FT
BO	BOTTOM WIDTH OF BREACH, FT
PPP	DEPTH (FT) OF EROSION PERPENDICULAR TO DOWNSTREAM FACE (KREG = 1)
	LENGTH (FT) OF BREACH ALONG DOWNSTREAM FACE (KREG = 2)
	BREACH WIDTH (FT) INCREASE (KREG = 3)
	ELEVATION (FT) OF TOP OF PIPE (KREG = 4)
HP	DISTANCE (FT) ERODED ACROSS TOP OF DAM (KREG = 1)
	VERTICAL DISTANCE (FT) ERODED AT UPSTREAM FACE (KREG = 2)
	DEPTH (FT) OF FLOW IN BREACH (KREG = 3)
	HEAD (FT) ON PIPE (KREG = 4)
TWD	TAIL WATER DEPTH, FT
DH	ESTIMATED EROSION DEPTH (FT) DURING TIME STEP
DHH	COMPUTED EROSION DEPTH (FT) DURING TIME STEP
KIT	ITERATION COUNTER
AGL	ACUTE ANGLE (DEG) THAT BREACH SIDE MAKES WITH VERTICAL

OTHER OUTPUT CONSISTS OF A HYDROGRAPH OF TOTAL OUTFLOW

THE FOLLOWING SUMMARY INFORMATION IS ALSO PRINTED OUT:

QPB	MAX OUTFLOW (CFS) THRU BREACH
TP	TIME (HR) AT WHICH PEAK OUTFLOW OCCURS
QP	MAX TOTAL OUTFLOW (CFS) OCCURRING AT TIME TP
TRS	DURATION (HR) OF RISING LIMB OF HYDROGRAPH (TP-TB)
TB	TIME (HR) AT WHICH FAILURE STARTS (EITHER KG = 2 OR KG = 4)
BRD	FINAL DEPTH (FT) OF BREACH
BRW	TOP WIDTH (FT) OF BREACH AT TIME TP

HU	ELEV (FT) OF TOP OF DAM
HY	FINAL ELEV (FT) OF RESERVOIR WATER SURFACE
HC	FINAL ELEV (FT) OF BOTTOM OF BREACH
AGL	ACUTE ANGLE THAT BREACH SIDE MAKES WITH VERTICAL AT T = TP
QO	OUTFLOW (CFS) AT T = 0.0
Z	SIDE SLOPE OF BREACH (FT/FT) AT TIME TP
TFH	TIME OF FAILURE (HR) DETERMINED BY SIMPLIFIED DAM-BREAK (SMPDBK) EQUATION
TFHI	TIME OF FAILURE (HR) DETERMINED BY INTEGRATION OF DISCHARGE TIME SERIES FROM TB TO TP
BO	BOTTOM WIDTH (FT) OF BREACH AT TIME TP

HU	ELEV (FT) OF TOP OF DAM
HY	FINAL ELEV (FT) OF RESERVOIR WATER SURFACE
HC	FINAL ELEV (FT) OF BOTTOM OF BREACH
AGL	ACUTE ANGLE THAT BREACH SIDE MAKES WITH VERTICAL AT T = TP
QO	OUTFLOW (CFS) AT T = 0.0
Z	SIDE SLOPE OF BREACH (FT/FT) AT TIME TP
TFH	TIME OF FAILURE (HR) DETERMINED BY SIMPLIFIED DAM-BREAK (SMPDBK) EQUATION
TFHI	TIME OF FAILURE (HR) DETERMINED BY INTEGRATION OF DISCHARGE TIME SERIES FROM TB TO TP
BO	BOTTOM WIDTH (FT) OF BREACH AT TIME TP